IJIRSET
International Journal of Innovative Research in
SCIENCE | ENGINEERING | TECHNOLOGY

e-ISSN: 2319-8753 | p-ISSN: 2347-6710


# INTERNATIONAL JOURNAL OF INNOVATIVE RESEARCH

## IN SCIENCE | ENGINEERING | TECHNOLOGY

Volume 12, Issue 5, May 2023

ISSN INTERNATIONAL STANDARD SERIAL NUMBER INDIA

Impact Factor: 8.423

9940 572 462 | 6381 907 438 | ijirset@gmail.com | www.ijirset.com

International Journal of Innovative Research in Science, Engineering and Technology (IJIRSET)

|e-ISSN: 2319-8753, p-ISSN: 2347-6710| www.ijirset.com | Impact Factor: 8.423| A Monthly Peer Reviewed & Referred Journal |

|| Volume 12, Issue 5, May 2023 ||

| DOI:10.15680/IJIRSET.2023.1202006 |

# Electromechanical System Coupling Dynamics under Variable Stiffness Factor and Moment Of Inertia

**Ferchichi Noureddine[1,2], Ben Aribia Houssem[1,3], Abid Slim[1,3], Masmoudi Sabeur [1,3], Ben Hmida Ghazi [1,3]**

Jazan University, Department of Electrical Engineering, College of Engineering, Saudi Arabia[1]

Tunis High National Engineering School, University of Tunis, Tunisia[2]

National Engineering School of Sfax, University of Sfax, Tunisia[3]

**ABSTRACT***:* In this paper, the coupling has been investigated in the dynamic behavior of a two-mass electromechanical system. In this system, mechanical perturbations like stiffness factor and moment of inertia lead to electromagnetic torque torsional vibrations. Then, by analyzing the impact of mechanical parameters on the torque ripple amplitude, solutions leading to a significant reduction of undesirable torsional vibrations are proposed.

**KEYWORDS***:* Electromechanical system, dynamic behaviour, stiffness factor, moment of inertia, electromagnetic torque, tortional vibrations.

## I. INTRODUCTION

The operation of electromechanical systems introduces frequent electrical and mechanical anomalies such as vibration problems, dynamic variations of electromagnetic torque, oscillations of currents, and speeds induced by external or internal factors in the system [1-2]. Thus, when several stresses act on the electrical and mechanical parts, nonconforming behaviors and premature failures will occur with exceeding the design limits.

There is a rapid development of electromechanical systems driven by electric motors, which requires deep knowledge of the dynamic interactions between electrical and mechanical parts. Among this knowledge is emphasized the importance of electromechanical coupling effects taken into account when possibly exact results are required for the study of extremely sensitive drive systems or for sufficiently precise and stable analyzes of their movements as well as for the development of active control algorithms for appropriate behavior [3]. In most cases, sufficiently accurate electromechanical models are generally not used due to the considerable simplifications of the mechanical system.

Moreover, as the definition of the term reminds us, a system is “a complex set of interacting elements”. This definition highlights the word interaction (coupling) which takes on particular importance in our context of study. Indeed, these couplings are also at the source of the electromechanical systems' complexity and can be present in the form of coupling between the elements, coupling between the disciplines, or couplings with the environment in which the system will evolve [4].

If we take an induction motor operating alone, when the rotor runs, its teeth will always turn relative to the stator teeth. Periodic variations in flux density will occur between the stator and rotor teeth, creating vibrations. Sometimes it can happen that these vibrations will start to resonate with the rotor's natural oscillations leading the motor to run very poorly [5-6-7]. A large number of researches have been conducted in this direction. Now if this motor with its problems presented above is integrated inside an electromechanical system, and other mechanical variables are added, the behavior of the induction motor becomes critical and requires solutions.

Nowadays, a severity of electromechanical interaction is commonly observed in the case of "variable speed drives" (VSD) of large rotating machines driven by synchronous or asynchronous motors controlled by load-switching inverters. Under transient and steady-state operating conditions, these devices are responsible for generating additional fluctuating torque components that can be a source of unexpected dangerous resonance effects of torsional vibration [8].

|e-ISSN: 2319-8753, p-ISSN: 2347-6710| www.ijirset.com | Impact Factor: 8.423| A Monthly Peer Reviewed & Referred Journal |

|| Volume 12, Issue 5, May 2023 ||

| DOI:10.15680/IJIRSET.2023.1202006 |

Torsional vibrations of electromechanical systems usually cause a large fluctuation in the rotor rotational speed of the motor. Such disturbances of the angular velocity superimposed on the average rotational speed of the rotor cause more or less severe variations in the electromagnetic flux and therefore additional oscillations of the electric currents in the motor windings.Then, the generated electromagnetic torque is also characterized by additional time-varying components that induce torsional vibrations of the driven electromechanical system [9, 10]. According to the above, the mechanical vibrations become coupled with the electrical vibrations of the rotor currents in the motor windings. The character of such coupling is often complicated and involves acute theoretical calculations [10].
Usually, vibrations are considered a harmful phenomenon. They can cause many adverse effects such as reduced operational efficiency of machines and vehicles, increased operating wear, or frequent increased risk of breakdowns. For these types of reasons, the issue of vibration reduction in electromechanical systems is still an intensely studied topic [11-13].

## II. ELECTROMECHANICAL STUDY MODEL

An electric drive is an electromechanical system (Fig. 1) intended to carry out a precise technological process. It consists of an electric motor, powered by a static converter or a generator, a control system, a mechanical transmission system, and a load. The electrical power supplied by the power source to the power converter is transformed into adjustable electrical power. The latter is transformed into electromagnetic and mechanical power by the motor. The motor is in fact an electromechanical converter whose rotor can be associated with the mechanical part of the electric drive. The mechanical power at the motor shaft is transmitted to the load via a mechanical converter.
The mechanical part of an electric drive constitutes in itself a complex system comprising the rotor of the motor, the transmission elements, and the working body. The structural elements of the electromechanical system exhibit a more or less complex interaction during operation. The simplified single-mass model, where the entire mechanical part is represented by its inertia, is commonly used in the literature devoted to electrical drives.But, in many cases of training, because of the finite rigidity of the connections between the different elements, it is important to make a representation in the multi-mass of the mechanical part. This makes it possible to highlight the influence of mechanical disturbances that can occur in these types of drives. For their analyses, the mechanical part is replaced by its equivalent calculation model. This allows them to be compared to determine which ones have the greatest influence on drive operation.

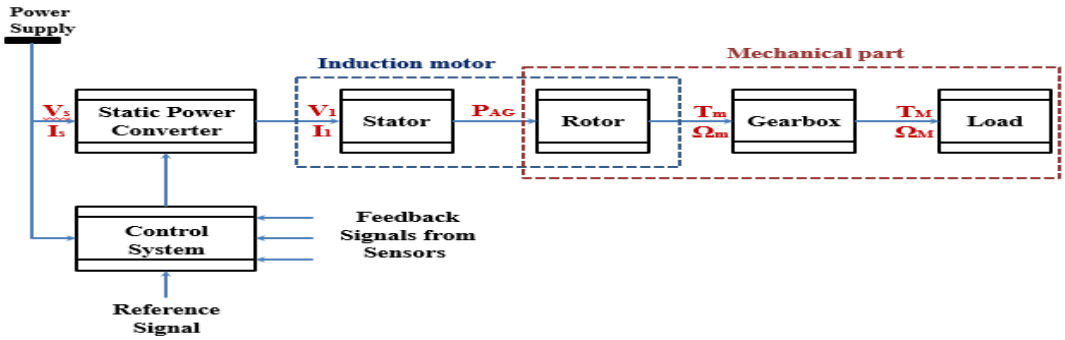


Fig. 1: Typical diagram of an electromechanical system

For the mechanical part, the equivalent model must be constituted by the elements which have a great influence on the drive operation (figure 2) and which carry out the same type of movement, rotation, or translation [14].The latter is referred to a previously chosen element whose movement is of the most interest and principle specification requirements. The reference principle of the equivalent diagram is based on the conservation law of energy, the kinetic and potential energies of the element before and after the reference must be equal.

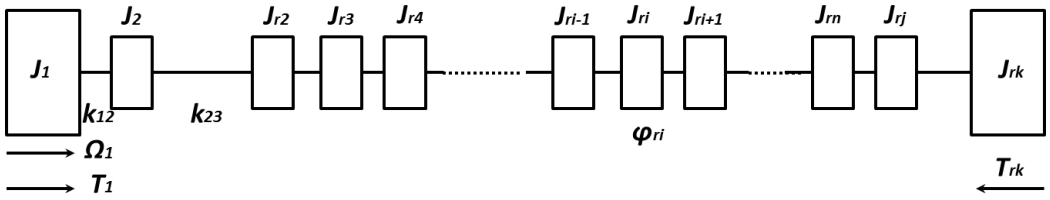


Fig. 2: Equivalent calculation diagram of an electromechanical drive

|e-ISSN: 2319-8753, p-ISSN: 2347-6710| www.ijirset.com | Impact Factor: 8.423| A Monthly Peer Reviewed & Referred Journal |

|| Volume 12, Issue 5, May 2023 ||

| DOI:10.15680/IJIRSET.2023.1202006 |

The mechanical part of the electromechanical system consists of several elements connected by often elastic connections. Fig. 2 presents the equivalent calculation diagram containing the parameters (moments of inertia $J_i$, stiffness factors $k_{i,i+1}$, angular velocities $\Omega_i$ or linear $V_i$, etc.), characterizing the movement of the rotor and all other moving parts of the electromechanical drive.

Considering the large number of elements and existing links between them, the equivalent calculation scheme becomes too complex, this complexity requires simplifications according to transformation rules. This is why parameters must be referred to a previously chosen element (very often the rotor of the electric motor is chosen as the reference element). This operation highlights the elements having the greatest influence (moment of inertia, stiffness coefficient, etc.) on the movement of the electromechanical drive.

Thus by referring the moment of inertia of the *i* element rotating at speed $\Omega_i$, to the speed $\Omega_1$, we have:

$$J_{ri}\frac{\Omega_1^2}{2} = J_i\frac{\Omega_i^2}{2} \tag{1}$$

We get the reference expression:

$$J_{ri} = J_i\frac{\Omega_i^2}{\Omega_1^2} = \frac{J_i}{i_{1i}^2} \tag{2}$$

Where:

$i_{1i} = \frac{\Omega_1}{\Omega_i}$ is the passing ratio from the reference shaft to the shaft *i* of the electromechanical system.

After these reference operations, the moment of inertia of the driven system (considering only the rotational movement) will be:

$$J_\Sigma = J_1 + \sum_{i=2}^{n}\frac{J_i}{i_{1i}^2} \tag{3}$$

Where *n* is the number of elements performing the rotational movement.

The equations describing the mechanical system are deduced from the following Lagrange motion model:

$$\frac{d}{dt}\left(\frac{dL}{d\dot{q}_i}\right) - \frac{dL}{dq_i} + \frac{dW_d}{d\dot{q}_i} = Q_i \tag{4}$$

Where $L = W_c - W_p$

$W_c$ : kinetic energy of the system.

$W_p$ : potential energy of the system.

$W_d$ : energy dissipated.

Using the expression for $L$ in (4), we get the following equation:

$$\frac{d}{dt}\left(\frac{dW_c}{d\dot{q}_i}\right) - \frac{d}{dt}\left(\frac{dW_p}{d\dot{q}_i}\right) - \frac{dW_c}{dq_i} + \frac{dW_p}{dq_i} + \frac{dW_d}{d\dot{q}_i} = Q_i \tag{5}$$

Since our study only concerns the rotational movement, we therefore have $q_i = \varphi_i$ , $\dot{q}_i = \Omega_i$ and $Q_i = T_i$.

$\varphi_i$ and $\Omega_i$ are respectively the displacement and the angular velocity of the element *i*. $T_i$ is the torque applied to element *i*.

So the generalized Lagrange equation becomes (for each system element):

$$\frac{d}{dt}\left(\frac{dW_c}{d\Omega_i}\right) - \frac{d}{dt}\left(\frac{dW_p}{d\Omega_i}\right) - \frac{dW_c}{d\varphi_i} + \frac{dW_p}{d\varphi_i} + \frac{dW_d}{d\Omega_i} = T_i \tag{6}$$

The following equations (7), (8), and (9) respectively represent the expressions of the kinetic, potential, and dissipated energies of a mechanical system with *n* masses in rotational motion:

|e-ISSN: 2319-8753, p-ISSN: 2347-6710| www.ijirset.com | Impact Factor: 8.423| A Monthly Peer Reviewed & Referred Journal |

|| Volume 12, Issue 5, May 2023 ||

| DOI:10.15680/IJIRSET.2023.1202006 |

$$W_c = \sum_{i=1}^{n} \frac{J_i \Omega_i^2}{2} \tag{7}$$

$$W_p = \sum_{i=1}^{n-1} \frac{k_{i,i+1}\left(\varphi_i - \varphi_{i+1}\right)^2}{2} \tag{8}$$

$$W_d = \sum_{i=1}^{n-1} \frac{\beta_{i,i+1}\left(\Omega_i - \Omega_{i+1}\right)^2}{2} \tag{9}$$

By introducing these last expressions into the generalized Lagrange equation, we obtain a mechanical model with *n* masses which is described by the following system of equations

$$\begin{aligned} &J_1.s.\Omega_1 + \frac{k_{12}}{s}(\Omega_1 - \Omega_2) + \beta_{12}(\Omega_1 - \Omega_2) = T_e - T_{r1} \\ &J_2.s.\Omega_2 + \frac{k_{12}}{s}(\Omega_1 - \Omega_2) + \frac{k_{23}}{s}(\Omega_2 - \Omega_3) - \beta_{12}(\Omega_1 - \Omega_2) + \beta_{23}(\Omega_2 - \Omega_3) = -T_{r2} \\ &J_n.s.\Omega_n - \frac{k_{n-1,n}}{s}(\Omega_{n-1} - \Omega_n) - \beta_{n-1,n}(\Omega_{n-1} - \Omega_n) = -T_{rn} \end{aligned} \tag{10}$$

Where:

$J_i$ : moment of inertia of $i^{th}$ mass.

$\Omega_i$ : angular speed of $i^{th}$ mass.

$C_{ri}$ : resistant torque applied to the $i^{th}$ mass.

$k_{i,i+1}$ : stiffness coefficient between $i^{th}$ and $i^{th}+1$ masses.

$\beta_{i,i+1}$ : damping coefficient between $i^{th}$ and $i^{th}+1$ masses.

After the multi-mass system equation based on the generalized model with *n* masses is carried out, we specify our study to a two-mass system which would therefore be described by the following system of equations

$$\begin{cases} J_1.s.\Omega_1 - \frac{k_{12}}{s}(\Omega_1 - \Omega_2) - \beta_{12}(\Omega_1 - \Omega_2) = T_e - T_{r1} \\ J_2.s.\Omega_2 - \frac{k_{12}}{s}(\Omega_1 - \Omega_2) - \beta_{12}(\Omega_1 - \Omega_2) = -T_{r2} \end{cases} \tag{11}$$

The system of equation (11) can be represented by the following Fig. 3, and from it, we can establish the structural diagram of the two-mass mechanical model as presented in Fig. 4.

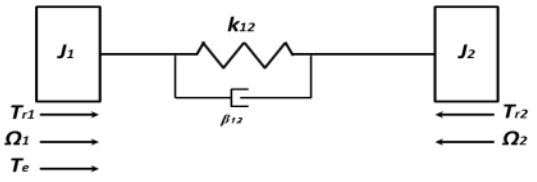


Fig. 3: Equivalent diagram with two masses

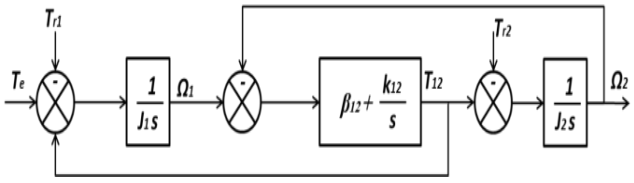


Fig. 4: Structural diagram of a two-mass mechanical system

The induction motor model is deduced supposing that the variables are expressed in a d-q reference frame rotating at synchronous speed with respect to the immobile reference frame $\alpha - \beta$ related to the stator [15]. Induction motor parameters in the reference frame $\alpha - \beta$ can be found using Park's direct transformation. To establish the two-phase motor model, it is assumed that:

- The motor windings are symmetrical.
- The magnetic circuit is not saturated.
- Voltages and currents are sinusoidal.

The induction machine equations expressed in a reference frame rotating at synchronous speed $w_s$ are:

|e-ISSN: 2319-8753, p-ISSN: 2347-6710| www.ijirset.com | Impact Factor: 8.423| A Monthly Peer Reviewed & Referred Journal |

|| Volume 12, Issue 5, May 2023 ||

| DOI:10.15680/IJIRSET.2023.1202006 |

$$\begin{cases} V_{ds} = R_s I_{ds} + s\Psi_{ds} - w_s \Psi_{qs} \\ V_{qs} = R_s I_{qs} + s\Psi_{qs} - w_s \Psi_{ds} \\ V_{dr} = R_r I_{dr} + s\Psi_{dr} - (w_s - w_r)\Psi_{qr} \\ V_{qr} = R_r I_{qr} + s\Psi_{qr} + (w_s - w_r)\Psi_{dr} \\ T_e = PL_{sr}(I_{qs} I_{dr} - I_{qr} I_{ds} \end{cases} \quad (12)$$

Where the magnetic equations are:

$$\begin{cases} \Psi_{ds} = L_s I_{ds} + MI_{dr} \\ \Psi_{qs} = L_s I_{qs} + MI_{qr} \\ \Psi_{dr} = L_r I_{dr} + MI_{ds} \\ \Psi_{qr} = L_r I_{qr} + MI_{qs} \end{cases} \quad (13)$$

and the stator and rotor currents are:

$$\begin{cases} I_{ds} = \dfrac{L_r \Psi_{ds} - L_{sr} \Psi_{dr}}{L_s L_r - L^2_{sr}} \\ I_{qs} = \dfrac{L_r \Psi_{qs} - L_{sr} \Psi_{qr}}{L_s L_r - L^2_{sr}} \\ I_{dr} = \dfrac{L_s \Psi_{dr} - L_{sr} \Psi_{ds}}{L_s L_r - L^2_{sr}} \\ I_{dr} = \dfrac{L_s \Psi_{dr} - L_{sr} \Psi_{ds}}{L_s L_r - L^2_{sr}} \end{cases} \quad (14)$$

Where:

$U_{ds}$ , $U_{qs}$ : Components of the stator voltages expressed in the reference frame $d-q$ ;

$I_{ds}$ , $I_{qs}$ : Components of the stator currents expressed in the reference frame $d-q$ ;

$I_{dr}$ , $I_{qr}$ : Components of the rotor currents expressed in the reference frame $d-q$ ;

$R_s$ : stator resistance;

$R_r$ : rotor resistance;

$L_s$ : stator inductance;

$L_r$ : rotor inductance ;

$L_{sr}$ : mutual inductance;

$P$ : number of pole pairs;

$T_e$ : electromagnetic torque ;

$\omega_s$ : angular synchronous speed;

$\omega_r$ : angular rotor speed ;

To describe the electromechanical system modeled with two masses, we combine equations (11) and (12), we will get two systems of equations after having replaced the derivative tool with the Laplace operator, and this is in order to facilitate the implementation of these equations in Matlab Simulink.

## III. SIMULATION OF ELECTROMECHANICAL SYSTEM

Regarding the choice of inertia, the inertia contribution of the motor in the total inertia of the system depends on the type of drive. In many drives, this contribution is quite high because of the reference to the motor of the parameters of most other moving parts.

|e-ISSN: 2319-8753, p-ISSN: 2347-6710| www.ijirset.com | Impact Factor: 8.423| A Monthly Peer Reviewed & Referred Journal |

|| Volume 12, Issue 5, May 2023 ||

| DOI:10.15680/IJIRSET.2023.1202006 |

The following Fig. 5 presents the simulation model of the two-mass electromechanical system based on an induction motor, there are three modules: the three-phase to two-phase transformation module, the induction motor, and the driven mechanical part.

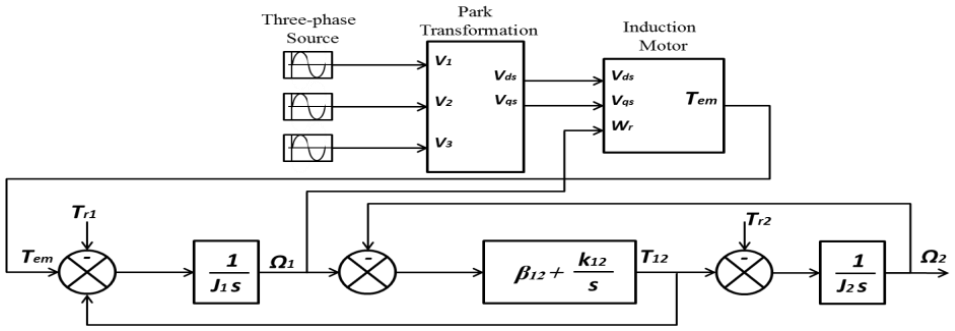


Fig. 5: Simulation model of two-mass electromechanical system based on an induction motor

The parameters of the simulated electromechanical system are presented in Table 1[16].

Table 1:Electromechanical system parameters

| $P_n$ kW | $V_s$ V | $I_s$ A | $T_n$ Nm | $R_s$ Ω | $R_r$ Ω | $L_s$ H | $L_{sr}$ H | $L_r$ H | p | f Hz | $J_1$ kg.m$^2$ | $J_2$ kg.m$^2$ | $k_{12}$ Nm/rad | $\beta_{12}$ Nms/rad |
|---|---|---|---|---|---|---|---|---|---|---|---|---|---|---|
| 2,2 | 120 | 12 | 12 | 0,6 | 0,4 | 0,061 | 0,059 | 0,061 | 2 | 60 | 0,01575 | 0,00175 | 20 | 0,001 |

The following figures represent the results found by simulation of the dynamic performance of the studied electromechanical system.

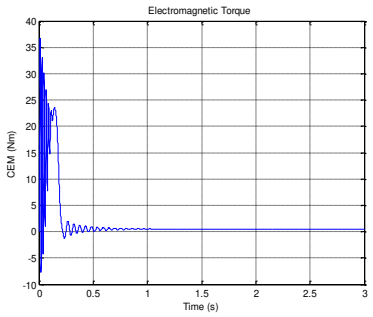


Fig. 6: Electromagnetic torque starting spectrum diagram

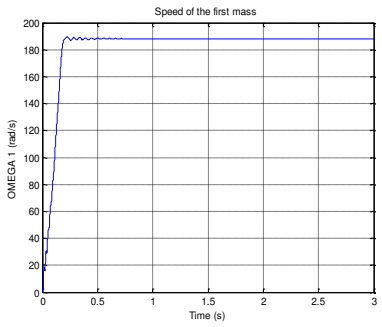


Fig. 7: Spectrum diagram at the starting speed of the first mass

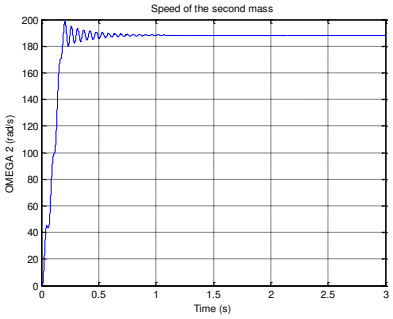


Fig. 8: Spectrum diagram at the starting speed of the second mass

The simulation results presented by the previous Figs. 6, 7, and 8 firstly show the validity of the two-mass electromechanical drive model based on an induction motor and highlight the starting state of the motor. It is considered, initially, that the load and resistant torques are zero with a unit gear ratio.

During the transient state, the electromagnetic torque is characterized by disturbing oscillations then it stabilizes after $0.3s$ . In terms of speeds, we note that the speed of the first mass has a ramp form and it stabilizes at a value close to that of synchronism, without forgetting to mention the presence of a few oscillations, especially at the beginning of starting. Since we consider a unity gear ratio, the speed range of the second mass remains equal to that of the first one. Nevertheless, we notice that the second mass amplitude of speed oscillations is greater than that of the first mass, this is due to the fact that the moment of inertia $J_1$ is greater than $J_2$. Consequently, by increasing the moment of inertia, the amplitude of oscillations decreases.

In what follows, we will apply a step-type load torque at the level of the second mass equal to *6 Nm*just at $t = 10s$ to see the behavior of the system.

|e-ISSN: 2319-8753, p-ISSN: 2347-6710| www.ijirset.com | Impact Factor: 8.423| A Monthly Peer Reviewed & Referred Journal |

|| Volume 12, Issue 5, May 2023 ||

| DOI:10.15680/IJIRSET.2023.1202006 |

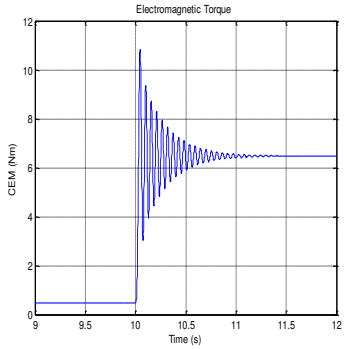


Fig. 9: Electromagnetic torque evolution following the application of a load torque

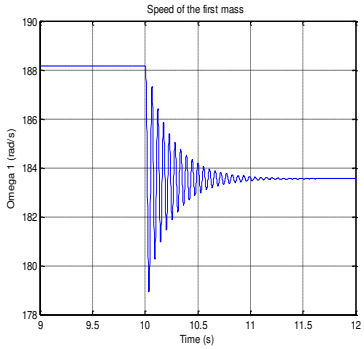


Fig. 10: First mass speed evolution following the application of a load torque

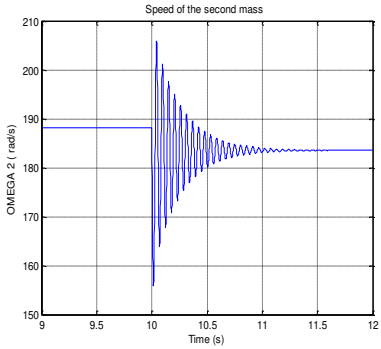


Fig. 11: Second mass speed evolution following the application of a load torque

It can be seen, that the application of a load torque is accompanied by the appearance of ripples in the electromagnetic torque and by a slight decrease in the two speeds. For both speeds, we also notice an increase in oscillations when applying a load torque. These oscillations are more important for the speed of the second mass because its inertia is low compared to that of the first one.

These findings highlight the difference between the “electrical” transient state and the “mechanical” transient state. Indeed, the transient state of "mechanical" origin is amortized much more slowly, this is due to the fact that, taking into account the inertia of the rotor, gearbox, and load, the speed of the system cannot vary instantly.

## IV. SIMULATIONRESULTS OF STIFFNESS FACTOR BETWEEN MASSES AND MOMENT OF INERTIA ON THE ELECTROMECHANICAL SYSTEM DYNAMICS

Generally, the use of a single-mass model, which assumes that the connection between its elements is infinitely rigid, does not highlight the dynamic properties of the electromechanical studied system. In order to remedy this problem, it is necessary to take into account the existing elasticity between the elements of the system. For this purpose, multi-mass modeling is essential. In our work, we adopt the two-mass model presented above.

It is important to point out that mechanical vibrations have a negative effect on the reliability and lifelong of the electromechanical systems in which they arise. In certain practical cases, the monitoring of these vibrations proves to be essential and makes it possible to avoid the degradation of the overall performances of the concerned processes.
We choose, in this first part, to analyze one of the main causes of mechanical vibrations in an electromechanical system based on an induction motor which is the stiffness coefficient which gives us an idea about the rigidity between masses $k_{12}$.To study its effect on the system response, the stiffness coefficient $k_{12}$ is varied while keeping all the other parameters constant.

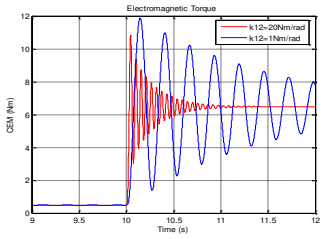


Fig. 12: Spectrum diagram of the electromagnetic torque after the application of a load torque Tr2 = 6 Nm at t = 10s, for different values of stiffness coefficient k12

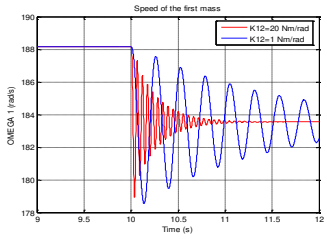


Fig. 13: Spectrum diagram of the first mass speed after the application of a load torque Tr2 = 6 Nm at t = 10s, for different values of stiffness coefficient k12

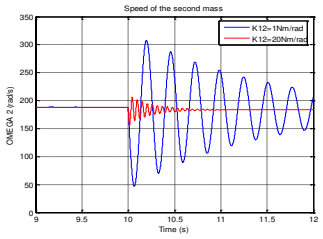


Fig. 14 : Spectrum diagram of the second mass speed after the application of a load torque Tr2 = 6 Nm at t = 10s, for different values of stiffness coefficient k12

First, we note that our two-mass system is subject to oscillations (mechanical vibrations), differently from the single-mass model, hence the interest in multi-mass modeling that allows us to really see the dynamic behavior of our

|e-ISSN: 2319-8753, p-ISSN: 2347-6710| www.ijirset.com | Impact Factor: 8.423| A Monthly Peer Reviewed & Referred Journal |

|| Volume 12, Issue 5, May 2023 ||

| DOI:10.15680/IJIRSET.2023.1202006 |

electromechanical system. Fig. 12 highlights the importance of oscillations during the application of load torque, we note that the greater the stiffness coefficient, these oscillations are better damped.
Curves in Fig. 13 represent the evolution of the speed of the first mass, this evolution is generated by significant oscillations, especially at the moment of load torque application. In addition, we note that these oscillations decrease by increasing the stiffness coefficient for the second mass.

The previous curves Fig. 14 clearly show that when the stiffness coefficient is increased, the oscillations generated by the speed of the second mass decrease. By comparing the speed shapes, we notice that the amplitude of oscillations for the second mass is greater than that of the first mass which has a higher inertia. So, to better study the electromechanical system dynamics, it is in our interest to vary the inertia $J_2$ and examine the effect of this variation on the amplitude of oscillations.

In this second part, we highlight the moment of inertia variation of the electromechanical system-driven part $J_2$, all other parameters remain constant including the inertia of the motor, in order to study the effect of this variation response on the system dynamic performances and especially the undesirable oscillations generated.
We present by the following Figs. 15, 16, and 17, the various shapes found by simulation of the electromagnetic torque and the two speeds for the first and second mass after changing the moment of inertia $J_2$ of the second mass.

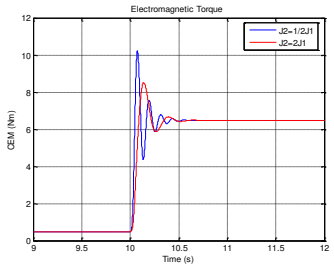


Fig. 15: Spectrum diagram of the electromagnetic torque after the application of a load torque Tr2 = 6 Nm at t = 10s, for different values of moment of inertia $J_2$

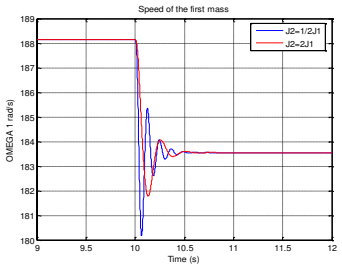


Fig. 16 : Spectrum diagram of first mass speed after the application of a load torque Tr2 = 6 Nm at t = 10s, for different values of moment of inertia $J_2$

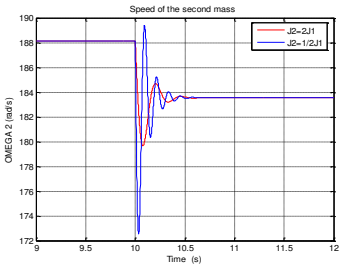


Fig. 17: Spectrum diagram of second mass speed after the application of a load torque Tr2 = 6 Nm at t = 10s, for different values of moment of inertia $J_2$

We notice from the previous figures that when the moment of inertia of the mechanical part becomes important compared to that of the motor, the oscillations are better damped. Also, we notice that the oscillation amplitudes are more important at the level of the second mass which is the source of the mechanical vibrations.

## V. CONCLUSION

In this paper, we have defined the multi-mass approach as a modeling principle, and we have exploited it to simulate the main parts of an electromechanical system. By simulating our system, we highlighted the phenomenon of mechanical vibration, which can take place. The transient state of electrical origin is dumped more quickly than that of mechanical origin, this is due to the effects of driven part-associated parameters. This phenomenon becomes more important when a load is suddenly applied.

To remedy these disturbances, we studied the importance of the stiffness coefficient between the masses as well as the contribution of the moments of inertia of the system's mechanical part. In order to minimize the amplitude peak of electromagnetic torque and second-mass speed, and improve the stability of the electromechanical system, simulation results highlight the positive effect of an increase in the stiffness coefficient associated with an increase in the driven mechanical part inertias. Thus, a damping of the mechanical resonance will be achieved as quickly as that of electrical origin and consequently, an optimization of the electromechanical system operation is envisaged.

|e-ISSN: 2319-8753, p-ISSN: 2347-6710| www.ijirset.com | Impact Factor: 8.423| A Monthly Peer Reviewed & Referred Journal |

|| Volume 12, Issue 5, May 2023 ||

| DOI:10.15680/IJIRSET.2023.1202006 |

## REFERENCES

[1] D. Wang et al. Electromechanical coupling dynamic characteristics of differential speed regulation system considering inverter harmonics under variable operating conditions. IEEE Access, vol. 10, 2022, pp. 12057-12069.
[2] T. Szolc, R. Konowrocki, M. Michajáow, and A. Prágowska, ''An investigation of the dynamic electromechanical coupling effects in machine drive systems driven by asynchronous motors,'' Mech. Syst. Signal Process., vol. 49, nos. 1–2, pp. 118–134, Dec. 2014.
[3] Y. A. Amer et al. Vibration analysis of permanent magnet motor rotor system in shearer semi-direct drive cutting unite with speed controller and multi-excitation forces. Applied mathematics and information science journal, vol. 3, 2021, pp. 373-381.
[4] Dasgupta, Kalyan , Kulkarni, A. M. , Soman, Shreevardhan. Studying Electromechanical Wave Propagation and Transport Delays in Power Systems. International Journal of Emerging Electric Power Systems, Volume 14, Issue 2, 2013, pp.105-114.
[5] L. Alberti and N. Bianchi. Theory and design of fractional-slot multilayer windings. Industry Applications, IEEE Transactions on, vol. 49, no. 2, pp. 841–849, 2013.
[6] M. Barcaro and N. Bianchi. Torque ripple reduction in fractional slot interior pm machines optimizing the flux-barrier geometries in Electrical Machines (ICEM), 2012 XXth International Conference on, 2012, pp. 1496–1502.
[7] G. Sizov, P. Zhang, D. Ionel, N. Demerdash, and M. Rosu. Automated multi-objective design optimization of pm ac machines using computationally efficient fea and differential evolution. Industry Applications, IEEE Transactions on, vol. 49, no. 5, pp. 2086–2096, Sept 2013.
[8] Ju J., Liu Y., Zhang C. Stability analysis of electromechanical coupling torsional vibration for wheel-side direct-driven transmission system under transmission clearance and motor excitation. World electric vehicle journal, vol. 13, no 46, 2022, pp. 1-14.
[9] Chen X., Chen R., Deng T. An investigation on lateral and torsional coupled vibrations of high power density PMSM rotor caused by electromagnetic excitation. Nonlinear dynamic journal, vol 99, 2020, pp, 1975–1988.
[10] Bouguenna I.F., Azaiz A., Tahour A., Larbaoui A. Robust neuro-fuzzy sliding mode control with extended state observer for an electric drive system. Energy, vol. 169, 2019, pp. 1054–1063.
[11] Tang, X., Yang W., Hu X., Zhang D. A novel simplified model for torsional vibration analysis of a series-parallel hybrid electric vehicle. Mechanical Systems and Signal Processing, Vol. 85, 2017, pp. 329–338.
[12] Shen C.R., Lu C.H. A refined torsional-lateral-longitude coupled vehicular driveline model for driveline boom problems. Appl. Math. Model., vol. 90, 2021, pp. 1009–1034.
[13] Zhang X.J., He W., Hu J.B. Impact of inertia control of DFIG-based WT on torsional vibration in drivetrain. IEEE Trans. Sustain. Energy, vol. 11, 2020, pp. 2525–2534.
[14] D. Łuczak, "Mathematical model of multi-mass electric drive system with flexible connection," 2014 19th International Conference on Methods and Models in Automation and Robotics (MMAR), 2014, pp. 590-595, doi: 10.1109/MMAR.2014.6957420.
[15] I.J. Ahmed, I. H. Husham. Mathematical driving model of three phase induction motors in stationary coordinate frame. Diyala journal of engineering science, vol. 8, no. 4, 2015, pp. 255-265.
[16] M. L. Doumbia et al. Comparative study of multi-mass models of electrical drives with asynchronous motors. Canadian journal of electrical and computer engineering, vol. 23, 1998, pp.107-112.

INNO SPACE
SJIF Scientific Journal Impact Factor

Impact Factor: 8.423

doi cross ref

ISSN INTERNATIONAL STANDARD SERIAL NUMBER INDIA

निस्केयर NISCAIR

# INTERNATIONAL JOURNAL OF INNOVATIVE RESEARCH

## IN SCIENCE | ENGINEERING | TECHNOLOGY

9940 572 462 6381 907 438 ijirset@gmail.com

www.ijirset.com

Scan to save the contact details